Soil Liquefaction: from mechanisms to effects on the built environment

Stefania Lirer
Università degli studi Guglielmo Marconi, Roma

Anna Chiaradonna & Lucia Mele
Università degli studi di Napoli Federico II

Introduction

Severe damages induced by soil liquefaction have occurred over time during some important earthquakes around the world (Anchorage, 1964; Niigata, 1964; Kobe, 1995; Kocaeli, 1999; Christchurch, 2010-2011; Emilia Romagna, 2012; Palu, 2018). The effects of liquefaction on structures in some of these areas were catastrophic, with large settlements and rotations of entire structural complexes leading to a loss of functionality and operative state. An accurate liquefaction hazard assessment (evaluation of soil susceptibility, assessment of the liquefaction potential for susceptible soils, and prediction of the effects) is therefore essential to protect life and safety, to reduce seismic risk of existing structures in a cost-effective manner, and to guide post-earthquake recovery.
Despite the experimental research efforts carried out in the last decades by many researchers to explain and understand the factors governing on liquefaction phenomena (cyclic liquefaction, cyclic mobility and flow liquefaction), major gaps still exist regarding the ability to accurately assess liquefaction effects on the built environment. The simplified procedures for liquefaction potential assessment, generally adopted in practice and suggested by codes, in some cases were not able to capture the observed severe damages induced by liquefaction phenomena observed after the major events, as for instance in the cases of the Canterbury earthquakes (New Zealand, 2010-2011) and of the 2012 Emilia Romagna seismic sequence.
The under prediction of liquefaction hazard highlighted that, despite research has significantly developed the state-of-art (SOA) on the soil liquefaction basic mechanisms, further progress remains to be made in the current state-of-practice (SOP) that continues to be largely empirical, using correlations based on earthquake case histories which neglect some relevant aspects (some of which addressed in this work) that rule the severity of liquefaction induced effects at ground level.

1. Some insights into the mechanisms

The term “liquefaction” has been used to describe phenomena (Robertson and Wride, 1998) associated with a rapid loss of soil shear strength and an accumulation of plastic strains due to the generation of excess pore water pressure in saturated soils subjected to earthquake shaking. The basic mechanisms ruling soil liquefaction have been deeply investigated in the last decades observing the stress-strain and pore-pressure generation behavior of saturated loose clean sands through undrained cyclic laboratory tests. Some of the main outcomes of these research studies are considered in the commonly used simplified methods for assessing whether earthquake-induced soil liquefaction may be triggered at a site. However, some advanced experimental results and new empirical evidences highlighted the relevance of some other aspects of the phenomenon, necessarily neglected at the laboratory scale, which should be incorporated in liquefaction assessment.

1.1 Seismic demand

Due to the irregularities and complexities of seismic loading (large ranges of frequencies, multidirectional propagation, Fig. 1a), it is very difficult to apply a representative loading condition to a soil specimen in laboratory tests. Uniform one-directional cyclic loading is commonly used in laboratory to evaluate soil resistance to earthquake induced liquefaction, superimposing the cyclic shear loading in the same direction of the "driving" static shear (if considered).

In recent years, significant experimental results carried out with un-conventional devices (multi-directional simple shear for level ground or sloping ground conditions) expanded the current understanding of soil liquefaction mechanisms and highlighted some areas in which the current theory and practice can be misleading or un-conservative. The pore water generation under by-directional shaking condition is higher than that measured under one-directional shakings and, as a consequence, the liquefaction resistance of soils under multi-directional simple shear conditions is lower. Under bi-directional "sloping ground" condition, the number of cycles to trigger liquefaction is significantly affected by the deviation between the driving shear stress and the superimposed undrained shear loading direction. If liquefaction is attained for a value of $r_{u,lim}$ approximately equal to 1.0 under uni-directional "level ground" loading conditions, the value of $r_{u,lim}$ could be significantly less than 1.0 (Fig.1b) for multi-directional sloping ground conditions. Again, the commonly used triggering criteria (stress based) would fail if applied to unconventional cyclic tests .

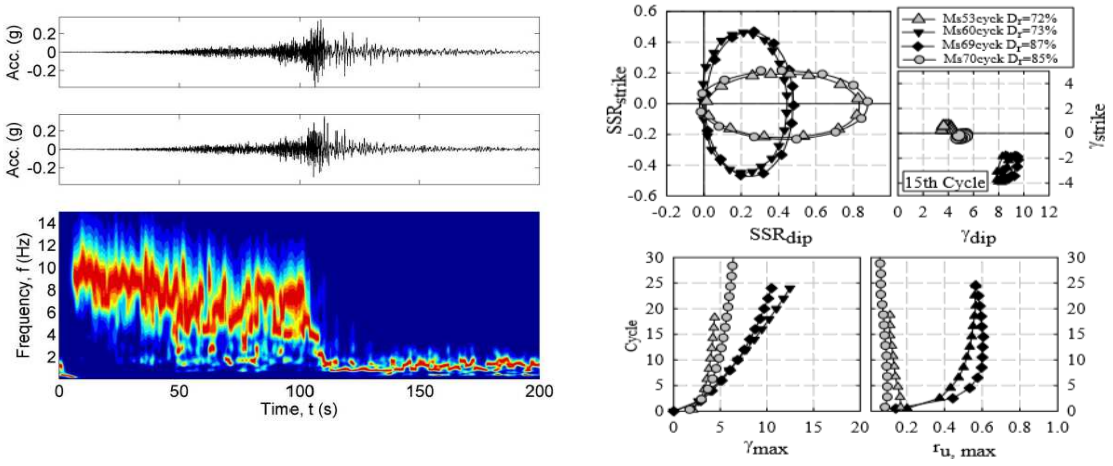

(a) (b)

Fig. 1. Horizontal ground surface time histories (a) and normalized Stockwell spectrogram for IBR014 site in 2011 Tohoku earthquake (Kramer & Greenfield, 2019); (b) results of bi-directional simple shear tests (Kammerer et al. 2004)

1.2 Liquefaction Triggering

Liquefaction initiation criteria are commonly based, at the laboratory scale, on a threshold defined in terms of either excess pore-pressure (r_u) or strain amplitude (ε_{DA}, γ_{DA}) within the specimen. The two criteria generally give the same results in loose sands and level ground loading condition, where the excess pore pressure is accompanied immediately by accumulation of large shear strains. Conversely,

denser sands or gravelly soils may generate high pore pressure under severe cyclic loading but they have limited shear strain potential due to their strong dilative behavior. Regarding strain based criteria, the influence of the selection of different strain levels and different deformation modes (e.g., triaxial or simple shear) on the measured liquefaction resistance or cyclic strength varies from relatively insignificant in loose soils to highly important in dense soils (Wu et al., 2004; Flora et al., 2012; Flora & Lirer, 2013). More interesting are the less known triggering criteria that use both cyclically induced stresses and strains as: apparent viscosity η (area bounded by the stress-strain rate hysteresis loops during cyclic loading) and energy dissipated per unit volume Es (area bounded by the stress-strain hysteresis loops during cyclic loading).

The apparent viscosity (Chen et al., 2006) is a physically based parameter able to represent the liquefaction induced change in the soil state, that switches from that of a solid to that of a viscous fluid. The relevance of the apparent viscosity can be clearly observed in Fig. 2a, were the results of cyclic triaxial tests carried out on reconstituted and undisturbed cohesionless soils (Lirer & Mele, 2019) are plotted: it can be noted that the decay of apparent viscosity is strictly related to the excess pore pressure build up. The experimental evidences showed that the constitutive models of the shear thinning non-Newtonian fluid (pseudo-plastic fluid) are able to reproduce the stress-strain rate relationship of the liquefied soils. Such models have been adopted by some researchers to simulate large deformation phenomena as lateral spreading or drag forces induced by liquefied soils on structures.

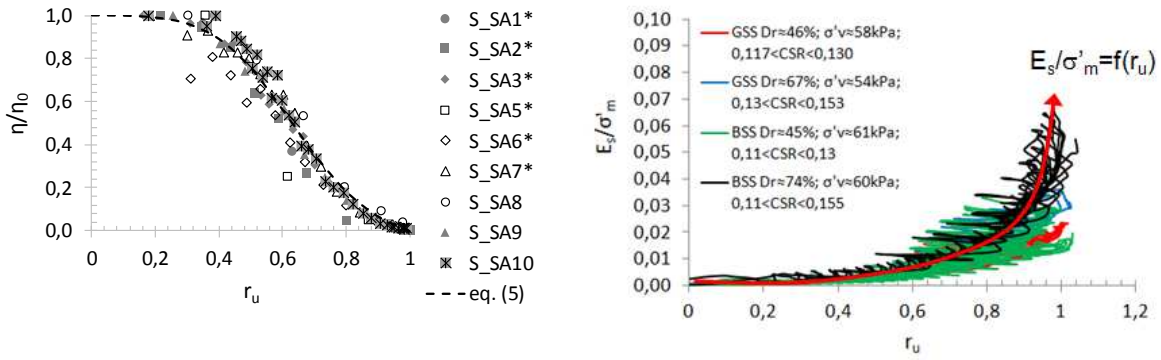

(a) (b)

Fig. 2. Normalized apparent viscosity η/η_0 (a) and normalized cumulative strain energy E_s/σ'_m (b) versus pore pressure ratio, measured in cyclic tests on saturated sandy soils (Lirer & Mele, 2019)

The cumulative dissipated energy (cumulative enclosed area of the stress-strain hysteresis loops) per unit volume is a useful index for the analysis of the cyclic behavior of soils because it is strongly correlated to the pore pressure build - up (Fig.2b). Several laboratory tests have demonstrated that, for a given soil, the total strain energy density required to induce liquefaction ($E_{s,liq}$, capacity energy) is independent of the applied load pattern (harmonic or irregular) and type of tests performed, mainly depending on few parameters representing soil state condition (σ'_m, D_r, S_r). In unsaturated soils, the specific energy of deformation needed to reach liquefaction can be seen as the sum of two components, the deviatoric energy and the volumetric energy: the last one can be computed - as the sum of three components (Mele et al., 2018, Mele & Flora 2019) - in undrained cyclic tests carried out in devices able to measure volumetric strains during the loading patterns.

2. Assessment of liquefaction potential

2.1 Simplified methods

In engineering practice, the evaluation of the potential for the occurrence of liquefaction is usually done by means of simplified approach (stress-based, strain-based and energy-based) in which, for each layer of liquefiable soil, the seismic demand is compared to the soil capacity considering level ground free field condition (FS_{liq}). The dominant approach used in practice is the stress-based one, because several semi-empirical correlations (Seed & Idriss, 1971; Idriss & Boulanger, 2006) derived from case history data have been developed for the calculation of the soil resistance to liquefaction (CRR) from in situ tests. Among them, the SPT and CPT based liquefaction correlations are the most reliable because they are supported by large databases on the occurrence of liquefaction.
The energy based approach is an alternative method of liquefaction assessment, in which the use of dissipated energy Es (previously introduced) as a measure of liquefaction resistance offers a number of advantages: it is related to both cyclic stresses and strains, is independent of the applied loading pattern, and allows to quantify, in a simplified way, the induced excess pore pressure (Azeiteiro et al. 2017). The key point in the energy based approach is the properly computation of the energy demand considering the effects of energy source and attenuation with distance (Kokuseho and Suzuki, 2011). Despite some empirical relationships have been proposed by many authors, the upward energy can be easily computed via an equivalent site response analysis.

2.2 Dynamic methods

Advanced constitutive models have been incorporated into non - linear dynamic response analyses, in order to provide a more rigorous approach to predict soil response (stress-strain and pore pressure) under a wide variety of loading conditions. In dynamic methods, excess pore water pressure can be estimated adopting two different approaches:
(1) a ‘decoupled’ approach, where the amount of excess pore pressure is computed adopting semi-empirical relationships using the results of a seismic response analysis in total stress;
(2) a ‘coupled’ approach that allows to compute the time history of excess pore water pressure carrying out non-linear dynamic analyses in effective stress by using either simplified or advanced soil constitutive models.

2.3 Liquefaction potential analysis for Pieve di Cento site: simplified vs dynamic methods

The liquefaction potential of a site located in Emila Romagna (Pieve di Cento, Fig. 3a) has been evaluated with the simplified energetic approach and via a 1D “loosely coupled” dynamic analyses, developed with the code SCOSSA (Tropeano et al., 2019) that adopts the simplified pore water pressure model developed by Chiaradonna et al. (2018). According to the energetic based approach, in each layer the energy capacity was compared to the energy demand . The energy demand (Fig. 3b) was quantified via a 1D

equivalent linear site response analyses (EERA, Bardet et al., 2000), in which soils properties have been calibrated on laboratory tests results and a ground motion input - compatible with the 20 May 2012 Emilia Earthquake - was imposed at the base of the 1D subsoil model. The energy capacity and the relationship between the cumulative strain energy dissipated in a unit volume (E_s/σ'_m) to the pore pressure ratio were determined by means of cyclic tests on reconstituted specimens of Pieve di Cento sand (Fig. 2b). Both liquefaction potential analyses show that soil liquefaction occurs in the deep liquefiable sandy layer (4.6<z<6 m), where the induced excess pore pressures reach the limit value (r_u≈1, Fig. 3c).

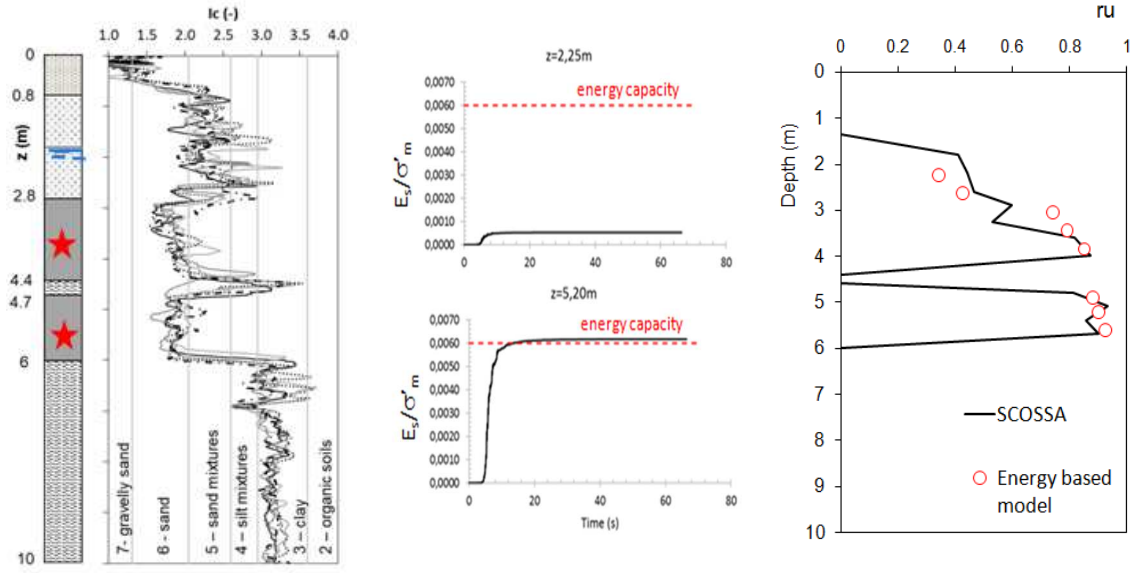

(a) (b) (c)

Fig. 3: Liquefaction potential analyses for the site of Pieve di Cento – trial field in LIQUEFACT project (a): comparison between pore pressure ratio computed via the simplified energy based analysis and via the 1D "loosely coupled" dynamic analysis (c)

3. Liquefaction hazard maps

In the last years, there has been an increasing awareness of the necessity to develop liquefaction micro-zonation maps in order to understand liquefaction induced hazard and manage the associated risk of damage to land and structures. Although a variety of ground failures may occur due to liquefaction (and some others may be triggered by pore pressure increase even before it), in the state of practice the liquefaction hazard maps are based on single "cumulative parameters" that somehow quantify the severity of all potential liquefaction induced effects at ground level. If the vulnerability parameter is well-calibrated and effective, it should well correlate to the observed damage datasets.

3.1 Cumulative Indexes of Liquefaction Potential

The first vulnerability indicator was introduced by the pioneering work of Ishihara (1985), where he highlighted the beneficial role of the upper non-liquefiable layer ("crust") in mitigating the damaging effects of liquefaction at ground surface.
The vulnerability of sites to liquefaction was also considered by Iwasaki (1982) that introduced a Liquefaction potential Index (LPI) which gives a measure of the vulnerability of sites to liquefaction effects. The contribution of all the liquefiable layers in the first 20 m of depth is calculated, weighted for a depth weighting factor linearly decreasing with depth.
An indicator more related to liquefaction damage at ground surface is the free field settlement indicator (S_{V1D}) defined by Zhang et al. (2002) for clean sands, because it is a direct measure of the amount of water expelled from the liquefiable layers when the volumetric consolidation occurs.
Following the 2010-2011 Canterbury earthquake series (New Zealand) that caused widespread liquefaction phenomena, the Liquefaction Severity Number (LSN) has been proposed by Tonkin and Taylor (2013): the parameter, due to the adoption of a hyperbolic depth weighting function (1/z) enhances the relevance of the shallower liquefiable layers to the overall damage.

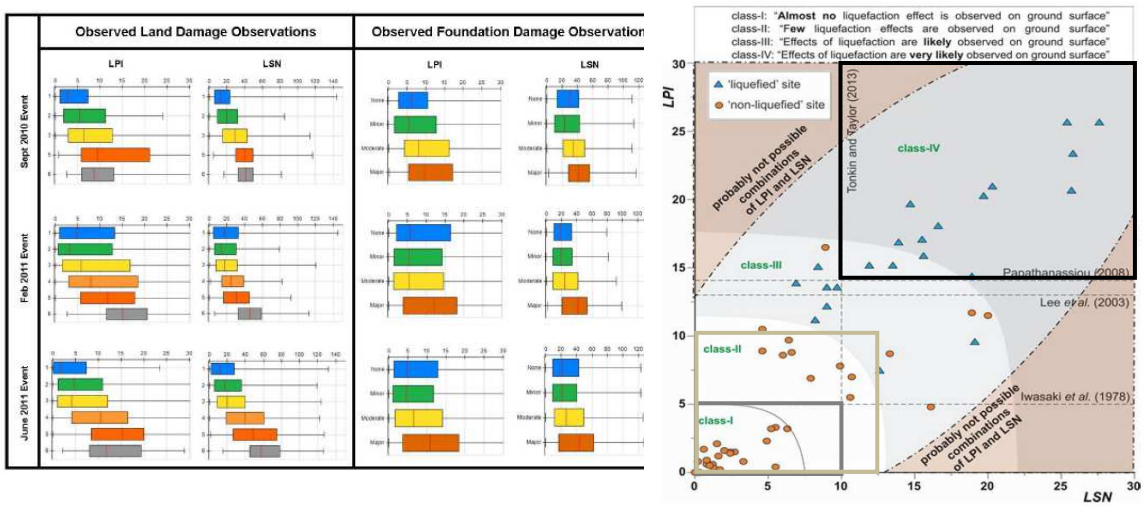

(a) (b)

Fig.4. Cumulative indexes LPI and LSN: a) land and foundation damages for Christchurch regions (b) correlation for case history data from Emilia Romagna region (Papathanassiou et al. 2015)

The correlation of the parameters LPI and LSN to measured damage datasets has been analysed by many authors (Fig.4). For the well - known 2010-2011 New Zealand sequence of earthquakes, for which an extensive damage mapping was done, the LPI correlation with land damage is event specific, while the LSN parameter appears to provide a more consistent correlation with observed damages datasets (Fig.4a) for all seismic sequences.

3.2 Induced dAmage Measurement I_{AM}

A new physically based cumulative index of liquefaction potential (Induced dAmage Measurement - I_{AM}), strictly related to the free field volumetric settlement induced by the dissipation of the excess pore

pressure developed in the shallow liquefiable layer, was introduced by the authors (Di Ludovico et al. 2019; Chiaradonna et al., 2019). The advantage of this new indicator is that it can be calculated with a rigorous calculation by means of dynamic analysis in effective stress (e.g., with SCOSSA) or in a simplified way by indirectly computing the values of ru through the application of a relationship with the safety factor against liquefaction FS_{liq} (Chiaradonna & Flora, 2019).
The effectiveness of this new cumulative index has been verified comparing it with the LSN indicator for a specific subsoil (Pieve di Cento, Fig. 3a) by means of 1D dynamic effective stress analyses, for a range of seismic inputs and maximum accelerations . The obtained trend for I_{AM} and LSN with the peak ground acceleration (a_{max}) is basically the same, confirming the reliability of the new vulnerability indicator. Even if for high values of a_{max}, the simplified approaches (r_u-FS_{liq}) gives an overestimation of I_{AM} values, the possibility to calculate the indicator without using dynamic analyses represents a further strength of the new indicator.

4. Effect of liquefaction on the built environment

The effects of soil liquefaction can take many forms in the environment: flow failures, lateral spreading, ground oscillation, loss of bearing capacity, settlements and increased lateral pressure on retaining walls. Severe structural damage induced by liquefaction has occurred over time during the major earthquakes. The effects of liquefaction on buildings can be catastrophic, with rotations of entire structural complexes leading to a loss of functionality and operative state.
Recently, centrifuge tests and advanced numerical modelling (e.g. Karamitros et al. 2013; Bray and Dashti 2014) showed that the presence of structures has an influence on the (3D) stress field and drainage pattern within the subsoil which significantly affects the potential for liquefaction triggering and therefore also the soil-foundation-structure interaction mechanism.

4.1 Soil settlements

The commonly observed significant sediment ejecta and building punching indicate that the effects of liquefaction are more severe than those expected based on the quantification of post-liquefaction volumetric free field reconsolidation settlements. Despite that, the state of practice for estimating liquefaction induced building settlements is largely based on empirical procedures developed to estimate the post-liquefaction 1D consolidation settlement in free field conditions (Zhang et al., 2002), neglecting important shear-induced deformation mechanisms, such as SSI ratcheting and partial bearing failure that contribute to building settlements.
Extending the pioneering work of Cascone and Bouckovalas (1999), a first simplified analytical methodology for the computation of liquefaction induced settlements of shallow footings on liquefiable soils with a clay crust has been proposed by Karamitros et al. (2013), based on the results of fully couples dynamic numerical analyses. The settlements have been correlated to the ground motion characteristics, to the post-shaking (degraded) bearing capacity of the footing and to the associated static safety factor (FS_{deg}).
More recently (Bray & Macedo, 2018; Karimi et al., 2018) 2D and 3D fully coupled non linear effective stress numerical analyses were performed in order to investigate the influence of all the involved

parameters on the performance of shallow founded structures (Fig. 5) and to develop an analytical expression for the computation of the shear induced building settlements.
The comparison between analytical predictions and experimental data (centrifuge and large scale shaking table tests, real case studies) highlighted that there is still an uncertainty in the robustness of such simplified analytical procedures for estimating liquefaction induced building settlements.

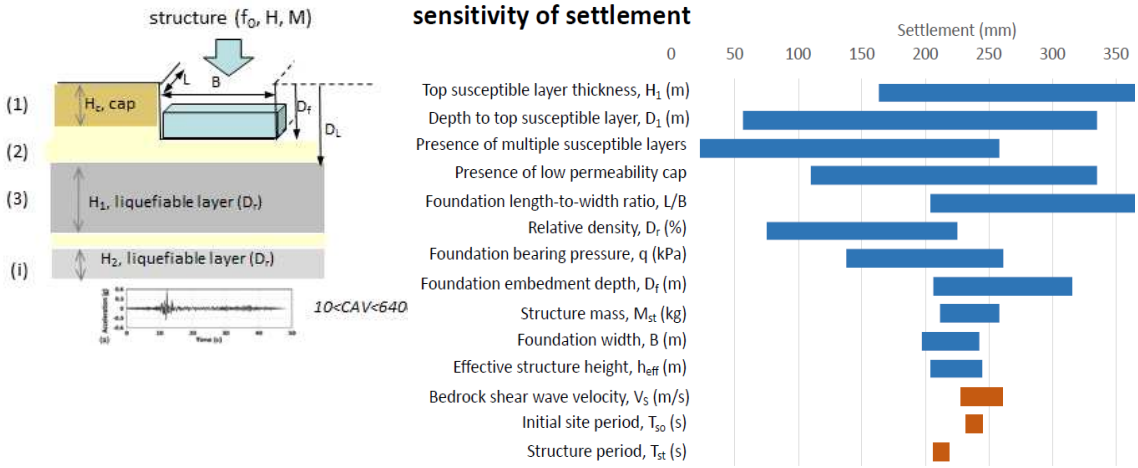

(a) (b)

Fig.5. Results of 3D (a) numerical study: sensitivity (b) of average permanent foundation settlements to input parameters (Karimi et al., 2018)

4.2 Lateral spreading

Lateral spreading involves permanent lateral displacement of large, superficial blocks of soil as a result of liquefaction of a subsurface layer. Displacements occur in response to the combination of gravitational forces and inertial forces generated by the earthquake: lateral spreads generally develop in gently sloping ground conditions and move toward a free face such an incised river channel, causing ground cracking that induce damage on foundations of buildings or structures and pipelines. Protection of existing and new structures and infrastructures requires a prediction of the potential for lateral spreading and for the associated displacements .
Lateral spreading is a complex process which is dependent upon a number of variables as the free face ratio (L/H), the ground motion characteristics, the thickness and depth of liquefied layer, topographic and geological boundary conditions. Although significant progress in understanding the mechanisms of lateral spreading has been made in the last years, in practice lateral spreading displacements are usually evaluated using a deterministic model and a single earthquake scenario and, as a consequence, they are very sensitive to the procedure adopted to select and model that scenario .
Youd et al. (2002) developed a regression-based predictive relationship starting from a large database of case histories, which takes into account soil properties, geometric variables and ground motion characteristics. Zhang et al. (2004) developed a cumulative strain-based model to predict permanent lateral displacements based on an estimate of the induced cyclic shear stress (estimated from CPT and SPT data), empirically corrected for geometrical effects such as free face ratio.
These empirical correlations are based on a limited case histories database of lateral spreading observations. Detailed back analyses of observations of some of these lateral spreading case histories

have demonstrated significant differences between the horizontal movements observed and the ones predicted with the empirical correlations .

5. Evaluation of structure vulnerability with fragility functions method

Seismic vulnerability assessment of structures or infrastructures in urban areas is a key component in liquefaction risk assessment for planning pre and post disaster strategies and policies. It defines the potential of a particular class of structures or infrastructures to be affected or damaged under a given ground motion event.
The structures (buildings, bridges, dams) vulnerability to soil liquefaction effects can be described by fragility curves which predict the probability of exceeding a specific damage level for a given value of a seismic severity parameter (e.g., liquefaction severity index or ground displacement). Depending on data resources, fragility functions can be generated either empirically, on the basis of observed damage data from past earthquakes, or analytically, based on the results of a large number of numerical analyses carried out introducing probabilistic distributions for some of the most relevant variables. In the last case, structural vulnerability can be evaluated via a simplified equivalent static procedure, where the free-field soil displacements (demand) are incrementally increased while the structural induced damage is numerically computed (generally neglecting the inertial forces). As a consequence, the fragility curves are specific to the considered structural configurations and damage variables, ground motions characteristic and soil conditions adopted in the numerical study.

5.1 Empirical fragility curves

Empirical fragility curves have been produced using observational damage data of masonry buildings collected after the 2012 Emilia earthquake in the municipalities of San Carlo and Mirabello (Di Ludovico et al., 2019), where widespread liquefaction phenomena were observed at ground level. Five damage grades (DG) were defined by accounting for the level and extension of the damage of the vertical components of the buildings. The damage grade has been subsequently correlated to the vulnerability parameter IAM, computed for both study areas based on the field investigation database produced by the Emilia Romagna region (166 CPTs and 170 CPTUs) assuming that the seismic event induced the full liquefaction of the shallow potentially liquefiable deposits. As a matter of fact, higher I_{AM} values are calculated along the paleo-channel of the Reno River in both municipalities, where most of the damaged buildings are also located. The empirical fragility curves showed that the new vulnerability index proposed by the authors is well related to the effects at ground level, therefore representing an effective preliminary tool to predict losses in liquefaction-prone areas.

5.2 Numerical fragility curves

An example of fragility curves for buildings affected by lateral spreading was developed (Somma et al., 2019) using the field measurements of permanent differential displacements obtained from ground survey after the 2010-2011 Canterbury sequence (Cubrinovski & Robinson, 2016). Case studies from the Canterbury sequence report major damage to buildings from differential lateral spreading, where the

structures were stretched due to the opening of cracks below them. Fragility curves were developed using a very simple structural scheme: a reinforced concrete frame with two isolated adjacent pillars, founded in a crust layer subjected to horizontal differential displacements. The structural capacity of one of the pillars (three limit states have been considered in terms of its flexural behaviour) was numerically computed with a simple 2D macro-element fixed at the top and loaded at the base by an horizontal force, quantified via a simple displacements – based spring model. For the considered failure mechanism and displacement demand (function of the distance from the waterway), the structural vulnerability assessment was done introducing randomness in both the parameters of the structural model as well in those of the geotechnical one, with assigned probabilistic distributions.

Concluding remarks

The analysis of liquefaction phenomena and of their consequences on the built environment remains one of the more active areas of research and development in geotechnical engineering.
"*The objective of the research should be to close the existing gap between states of the art SOA and state of practice SOP (Kramer, 2019)*". Both SOA and SOP should therefore develop in a more integrated manner, with the final goal of developing more comprehensive and reliable, but easy-enough-to-use, vulnerability assessment methods able to quantify liquefaction land damage and to evaluate the associated consequences for buildings and infrastructures.

References

Azeitero R.J.N., Coelho P.A.L.F., Taborda D.M.G. and Grazina J.C.D. (2017). *Energy-based evaluation of liquefaction potential under non-uniform cyclic loading*. Soil Dynamics and Earthquake Engineering (92): 650-665.

Bardet J.P., Ichii K. and Lin C.H. (2000). *EERA – A computer program for Equivalent-Linear Earthquake site response analysis of layered soil deposits*. Department of Civil Engineering, University of Southern California, USA.

Boulanger R.W. and Idriss I.M. (2016). *CPT-Based Liquefaction Triggering Procedure*. Journal of Geotechnical and Geoenvironmental Engineering, 142(2):04015065.

Cascone E. and Bouckovalas G. (1999). *Seismic bearing capacity of footings on saturated sand with a clay cap*. Proc. 11th European Conference on Earthquake Engineering.

Chen Y.M., Liu H.L. and Zhou Y.D. (2006). *Analysis on flow characteristics of liquefied and post-liquefied sand*. Chinese Journal of Geotechnical Engineering 28(9): 1139-1143.

Chiaradonna A., Tropeano G., d'Onofrio A. and Silvestri F. (2018). *Development of a simplified model for pore water pressure build-up induced by cyclic loading*. Bulletin of Earthquake Engineering 16(9):3627–3652.

Chiaradonna A. and Flora A. (2019). *On the estimate of seismically-induced pore water pressure increments before liquefaction*. Geotechnical letters. *Under review*.

Chiaradonna A., Lirer S., Flora A. (2019). *A damage-based liquefaction potential index for microzonation studies.* Engineering geology. Under review.

Di Ludovico M., Chiaradonna A., Bilotta E., Flora A. and Prota A. (2019). *Empirical damage and liquefaction fragility curves from 2012 Emilia Earthquake data*. Earthquake Spectra. *Under review*.

Facciorusso J., Madiai C. and Vannucchi G. (2016). *The 2012 Emilia earthquake (Italy): geotechnical characterization and ground response analyses of the paleo-Reno river levees.* Soil Dynamics and Earthquake Engineering 86: 71-88.

Flora A., Lirer S. and Silvestri F. (2012). *Undrained cyclic resistance of undisturbed gravelly soils*. Soil Dynamics and Earthquake Engineering (43): 366-379.

Flora A. and Lirer S. (2013). *Small strain shear modulus of undisturbed gravelly soils during undrained cyclic triaxial tests.* Geotechnical and Geological Engineering 31(4): 1107-1122.

Idriss I.M. and Boulanger R.W. (2006). *Semi-empirical procedures for evaluating liquefaction potential during earthquakes.* Soil Dynamic and Earthquake Engineering (26): 115-130

Iwasaki T., Arakawa T. and Tokida K. (1982). *Simplified procedures for assessing soil liquefaction during earthquake*. Proc. Conference of Soil Dynamic and Earthquake Engineering, Southampton, UK; 925-939.

Kammerer A., Wu J., Riemer M., Pestana J. and Seed R. (2004). Shear strain development liquefiable soil under bi-directional loading conditions. Proc. 13th World Conference on Earthquake Engineering, Vancouver (Canada), 1-6 August 2004.

Karamitros D.K., Bouckovalas G.D. and Chaloulos Y.K. (2013). *Seismic settlements of shallow foundations on liquefiable soil with a clay crust.* Soil Dynamics and Earthquake Engineering (46): 46-76.

Karimi Z., Dashti S., Bullock Z., Porter K. and Liel A. (2018). *Key predictors of structure settlement of liquefiable ground: a numerical parametric study*. Soil Dynamic and Earthquake Engineering (113): 286-308.

Kokusho T. (2013). *Liquefaction potential evaluation: energy based method versus stress-based method.* Canadian Geotechnical Journal (50): 1088-99.

Kramer S.L. and Greenfield M.W. (2019). *The Use of numerical Analysis in the interpretation of liquefaction Case Histories.* Proceedings of the 7th International Conference on Earthquake Geotechnical Engineering, 7ICEGE, 17-20 giugno 2019, Rome (Italy)

Lirer S. and Mele L. (2019). *On the apparent viscosity of granular soils during liquefaction tests*. Bulletin of Earthquake Engineering. *Under review*.

Macedo J. and Bray J.D. (2018). *Key trends in liquefaction induced building settlements.* Journal of Geotechnical and Geoenvironmental Engineering 144 (11).

Mele L., Tan Tian J., Lirer S., Flora A., Koseki J. (2018). *Liquefaction resistance of unsaturated sands: experimental evidence and theoretical interpretation*. Géotechnique. DOI: 10.1680/jgeot.18.p.042.

Mele L. & Flora A. (2019). *On the prediction of liquefaction resistance of unsaturated sands.* Soil Dynamics and Earthquake Engineering.

Mele L., Lirer S., Flora A. (2019). *The specific deviatoric energy to liquefaction in saturated cyclic triaxial tests*. 7th International Conference on Earthquake Geotechnical Engineering, 7ICEGE, Rome (Italy), 17-20 June 2019.

Robertson P.K. and Wride C.E. (1998). *Evaluating cyclic liquefaction potential using the cone penetration test*. Canadian Geotechnical Journal (35): 442-459.

Wu J., Kammerer A.M., Riemer M.F., Seed R.B. and Pestana J.M. (2004). *Laboratory study of liquefaction triggering criteria*. Proc. 13th World Conference on Earthquake Engineering. Vancouver (Canada), August 1-6.

Papathanassiou G., Mantovani A., Tarabusi G., Rapti D. and Caputo R. (2015). *Assessment of liquefaction potential for two liquefaction prove areas considering the May 20, 2012 Emilia (Italy).* Earthquake Engineering Geology (189): 1-16.

Seed H.B. and Idriss I.M. (1971). *Simplified procedure for evaluating soil liquefaction potential.* Journal of Soil Mechanics and Foundation Division (97): 1249-74.

Somma F., Millen M., Bilotta E., Flora A. and Viana da Fonseca A. (2019). *Vulnerability assessment of RC building to lateral spreading*. Bulletin of Earthquake Engineering. *Under review*.

Tonkin and Taylor (2013). Canterbury Earthquakes 2010 and 2011. Land report as at 29 February 2012 108 pp. Earthquake Commission.

Tropeano G., Chiaradonna A., d'Onofrio A. and Silvestri F. (2019). A numerical model for non-linear coupled analysis on seismic response of liquefiable soils. Computers and Geotechnics 105: 211-227.

Van Ballegooy S., Malan P., Lacrosse V., Jacka M.E., Cubrinovski M., Bray J.D., O'Rourke T.D., Crawford S.A. and Cowan H. (2014). *Assessment of liquefaction-induced land damage for Residential Christchurch*. Earthquake Spectra 30 (1): 31-55.

Youd T.L., Hansen C.M. and Barlett S.F. (2002). *Revised multi-linear regression equation for prediction of lateral spread displacements*. Journal of Geotechnical and Geoenvironmental Engineering 128 (12): 1007-1017.

Zhang G., Robertson P-K. and Brachman R.W-I (2002). *Estimating liquefaction-induced lateral displacements using the Standard Penetration Tests pr Cone Penetration Test*. Journal of Geotechnical and Geoenvironmental Engineering 861-871.

Zhang J., Huo Y., Brandenberg S. and Kashighandi P. (2008). *Effects of structural characterizations on fragility functions of bridges subject to seismic shaking and lateral spreading*. Earthquake Engineering and Engineering vibration (7): 369-382.